5. É. B. Georg and M. I. Yakushin, "Thermal boundary layer in models breaking down under a high-enthalpy gas flow," Izv. Akad. Nauk SSSR, Mekh. Zhidk. Gaza, No. 1, 26-31 (1976).
6. É. B. Georg and M. I. Yakushin, "Measurement of the concentration profile of cyanogen in a thermal boundary layer on models breaking down under a heat flow," Izv. Akad. Nauk SSSR, Mekh. Zhidk. Gaza, No. 3, 139 (1976).

COLLAPSE OF A SPHERICAL CAVITY, INDUCED BY AN UNDERWATER SPARK, NEAR A SOLID WALL

V. A. Burtsev and V. V. Shamko

UDC 532.528

A knowledge of the laws of the physical processes accompanying the collapse of cavities, formed by an underwater spark, in the presence of asymmetric boundary conditions is very important for a proper understanding of the causes responsible for the phenomena. We know, for instance, that neglect of the flow energy in the dynamic calculation of structures for impact loading of the explosion type can lead in several cases to overestimation of the theoretical source energy by a factor of two [1, 2]. In addition, a clarification of this question will lead to improvement in the technology of electric pulse processes in water [3].

The few theoretical [4-9] and experimental [10-13] investigations of the effect of a solid wall on the collapse of a spherical cavity in a liquid medium indicate deformation of the cavity, the formation of a liquid jet in the direction of the wall at the concluding stage of collapse, and consequent damage to the wall under certain conditions [9-13]. The proximity of the wall is also the reason for the translational movement of the cavity or its center toward the wall.

In some theoretical studies [5, 6], spherical collapse of a cavity has been considered, and the quantitative characteristics of the process obtained for this case have been used in some calculations [14]. Kling et al. [13] made a thorough experimental investigation of the quantitative picture of the effect of an adjacent solid surface on the collapse of spark-induced bubbles, but their experiments were conducted in a flow of liquid, i.e., in the presence of another additional source of asymmetry — the slip of the bubble in the flow, which leads to a significant change in the nature of cavity collapse [4, 9, 15].

The aim of the present work was an experimental verification of the applicability of the available experimental models for a description of the dynamics of collapse of a spherical vapor—gas cavity (VGC), formed by an underwater spark, near a plane solid wall.

1. Description of Experimental Apparatus and Methods of Investigation. The experiments were conducted in a special tank (1500 × 1000 × 500 mm) filled with distilled water. The tank was furnished with two Plexiglas windows, which enabled us to photograph the process in transmitted light from a powerful source. The solid wall was a square Viniplast sheet 20 mm thick, whose linear dimensions exceeded the maximum cavity diameter by a factor of more than two. The wall surface was set perpendicular to the free surface of the liquid. The gas cavity was formed by an underwater spark produced by the discharge of a 1-μF capacitor bank across a 10-mm spark gap. The charging voltage was 25 kV and the circuit inductance was 3 μH. The stability of the discharge (and, accordingly, of the parameters of the induced bubble) was maintained by straightening of the spark channel with a Constantan wire (diameter 0.003 mm) and by natural degassing of the liquid. The electrodes consisted of two copper needles of diameter 4 mm. The discharge took place at a depth of 240 mm, so that even in the case of a bubble of maximum radius (53 mm) the free surface had no effect on its motion

Nikolaev. Translated from Zhurnal Prikladnoi Mekhaniki i Tekhnicheskoi Fiziki, No. 1, pp. 80-90, January-February, 1977. Original article submitted January 12, 1976.

[16]. The normalized distance to the wall b_0^* (the ratio of the initial distance of the center of the VGC from the wall to its maximum radius $b_0^* = b_0^*/R_{max}$) was made equal to $b_0^* =$ 0.6, 0.7, 0.8, 1.05, 1.1, 1.6, 2.2, and 5.5. The process was photographed with an SFR-2M high-speed camera operating under frame-scanning conditions at a rate of $(1.5\text{-}30)\cdot10^3$ frames/sec. The range of speeds of the SFR-2M camera was enlarged by the use of a special attachment that greatly reduced the rate of rotation of the mirror [17]. The rate of rotation of the mirror was measured by recording the pulse repetition rate from a photosensor from the Lissajou figures with the aid of an S1-16 oscilloscope.

2. Results of Motion-Picture Observations. Figure 1 shows a series of frames demonstrating the collapse of a VGC formed by an underwater spark at different distances from the wall [$b_0^* = 5.5$ (a), 2.2 (b), 1.6 (c), 1.1 (d), 0.8 (e), and 0.6 (f)]. The time between frames in all cases was the same and equalled $\Delta t = 0.76$ msec [dimensionless time $\Delta\tau = \Delta t(p_\infty/\rho_\infty)^{1/2}/R_{max} = 0.143$]. It is apparent that during the collapse of a bubble at a distance $1.1 \leq b_0^* \leq 2$ from the wall it loses its initial spherical shape. The cavity becomes extended along a normal to the wall and acquires an ovoid shape.

The formation of an ovoid cavity at $b_0^* \leq 2$ indicates a low flow strength on the side of the plane. Hence, the pressure difference existing at the start of collapse ($\Delta p \sim 1$ atm) is not sufficient to tear the water away from the wall. Specially conducted experiments with a nonwettable solid wall (of Ftoroplast) at the same Δp did not show any appreciable difference in the picture of the process.

The rear (farthest from the wall) boundary cavity acquires a higher velocity than the other regions. Surface disturbances occur on it and lead to shape instability and the formation of a cumulative jet of liquid. The appearance of the jet was indicated by the crumpling and destruction of the spherical profile of the cavity.

The reasons for deformation of the VGC are quite understandable from the qualitative aspect. Not only capillary forces, but also forces of hydrodynamic origin act on the bubble surface. The introduction of asymmetry by the close solid surface alters the configuration of the hydrodynamic field. On the plane side the liquid flow is weakened, and at a number of peripheral points the hydrodynamic forces increase considerably and greatly exceed the surface-tension forces. In this case the spherical shape of the bubble (if it is still spherical at the time of attainment of maximal volume in the initial expansion), which owes its existence to surface tension, becomes unstable, and the bubble becomes capable of deformation, as distinct from the corresponding process in an unbounded liquid.

It is of interest to note that when $b_0^* < 1.1$ the cavity collides with the wall at the collapse stage, and when $1.1 \leq b_0^* < 1.6$ the collision occurs at subsequent stages of expansion. If $b_0^* \geq 1.6$, the collapsing cavity subsequently approaches the wall, but does not come in contact with it. Hence, when the VGC is at a distance of $b_0^* = 1.6$ or more from the wall the probability of damage to the wall is greatly reduced [13]. This is confirmed experimentally by the established fact of increase in the effectiveness of removal of molding materials from castings when a discharge on the casting is used [18].

We note that in the contraction period the cavity is a figure of revolution (which was indicated by passage of the highlight through the center of the VGC and also by the change in the light spot visible through the cavity in time with the change in shape of the cavity), whereas during repeated pulse cycles it had no regular geometric shape. The cavity at these stages became optically opaque, diffusely reflecting and absorbing the light flux incident on it. This picture was observed both in the presence and absence of the solid wall. This experimental fact is further evidence of asymmetric collapse of the initially spherical VGC. The high-speed microjets appearing at the moment of collapse of the cavity break it up into numerous small bubbles, whose subsequent development, like the phenomenon as a whole, is due to their effect on one another [16, 19]. In fact, in the case of slow flows around bodies the secondarily formed cavities retain their transparent surface [15]. With the approach of the VGC to the wall the onset of shape instability occurs earlier.

When $b_0^* \simeq 1$ a spherical bubble cannot form near the wall, i.e., the surface starts to become unstable at the moment of formation (see Fig. 1e). In this case the front boundary of the cavity becomes flat (like the wall itself) and remains so until it collides with the wall. A further reduction in b_0^* ($0.6 \leq b_0^* \leq 1.05$) leads to even greater deformation of the cavity; the front part is cut off, as it were, and has the shape of a spherical segment with a height slightly exceeding the equivalent (according to the area of the shadow photograph)

radius R*. The value of b_0^* in such cases was determined as the ratio b_0^*/R^*. The front boundary of the cavity at the growth stage reached the wall only when $b_0^* = 0.6$; the formed cavity was dome-shaped and remained like this for $t \leq 0.8T_-$ (see Fig. 1f, T_- is the time of collapse of the cavity). The nature of the collapse of such cavities differs from the model [16] for a hemispherical bubble on a wall. Initially the collapse in a plane parallel to the wall is a little more rapid, and only near the minimum is there a sharp increase in velocity along a normal to the wall. For instance, at the moment of formation of the jet ($t = 0.83T_-$), determined from the start of crumpling of the rear boundary of the VGC, the velocity of the boundary at the point of entry of the jet is 85-100 m/sec. We must infer that the jet velocity will be a little greater than the indicated values, since its passage into the cavity was not detected owing to the predominant reflection of the light beam by the spherical VGC surface. The maximum jet velocity recorded in the conducted experiments was about 150 m/sec for $b_0^* = 1.1$.

For a thorough investigation of the initiation and passage of the jet into the cavity a "thin" flat cavity was created in the direction of the light beam, as in [11], for instance. Such an approach, however, does not guarantee against the additional influence of a number of boundary effects [12], whose consideration is beyond the scope of the present investigation. In weightless conditions [15] the collapse of a cavity near a wall is similar to that discussed above. Hence, gravitational forces do not have a significant effect on the collapse of a VGC near a solid surface and their omission in the equation of motion (as in the theoretical models in [4-8]) is justified.

3. Effect of Wall on Deformation of Cavity. The outlines of the VGC surface at various times for two distances from the wall are shown in Fig. 2. The bottom is the side of the cavity nearest the wall. The outline of the cavity was determined by projecting its shadow photographs onto a screen with the necessary magnification. For comparison we used the theoretical calculations (dashed-dot lines) of Voinov (Fig. 2a, $\tau = 0$, 0.62, 0.82, 0.99), Shima (Fig. 2b, $\tau = 0$, 0.6, 0.8), Mitchell (Fig. 2c, $\tau = 0$, 0.6, 0.8, 0.87) for $b_0^* = 1.5$ (the experiment was conducted at $b_0^* = 1.6$), and Kling's experimental data (Fig. 2d, $\tau = 0$, 0.73, 0.9, 1) for $b_0^* = 1.14$. In view of the arbitrary choice of times $\tau = t\sqrt{p_\infty/\rho_\infty}/R_{max}$, characterizing the corresponding VGC outlines, there is some spread at the compared times. The maximum spread, however, did not exceed 5%.

An analysis of Fig. 2 shows that in all the considered cases the bubbles at the early stage of collapse ($\tau \leq 0.6$) are quasispherical and there is good agreement between the experimental and theoretical profiles. The experiment shows a greater relative elongation of the cavity along the normal to the wall than was the case in [7, 9, 13]. The greater disagreement of the obtained results with the data of [13] is probably due to additional asymmetry — slipping of the bubbles in the liquid flow — and to the difference in the pressure gradients at the phase interface at the initial instant of collapse. For the same reason Kling and Hammitt [13] found practically no shift of the front boundary during its collapse.

The front boundary of the cavity near the minimum acquires a higher velocity and moves away from the wall even when $b_0^* = 1.1$. It is characteristic that in the course of collapse the cavity again becomes spherical and only then, in view of the dominant velocity of the rear boundary, it is destroyed by the formed jet of liquid. For $b_0^* = 1.1$, beginning at $\tau = 0.7$, a dent, due to inflow of liquid into the VGC, is formed on the rear side of the cavity. This was indicated by the flat profile of this part. The jet attains its maximum velocity (150 m/sec) when the bubble reaches its minimum.

The appreciable movement of the front boundary of the cavity at the concluding stage of collapse is probably due to the cumulative effect when the front surface of the cavity attains its critical curvature, which is confirmed by the absence of such movement in the case where the front boundary of the cavity has minimum curvature (see Fig. 1e).

The greatest disagreement in cavity outlines was found between the data of the present experiment and the numerical calculations of Voinov (see Fig. 2a) and Shima (see Fig. 2b). This indicates a large error in models using flow potentiality for the kinematic description of the collapse of a VGC induced by an underwater spark near a solid wall. In addition, owing to the increasing deformation of the bubble the employed expansions in Legendre polynomials rapidly become unsuitable. The marker-and-cell technique is more accurate in this respect, although the degree of correspondence of the concluding stages of cavity collapse cannot be tested owing to cessation of the count at $\tau = 0.873$

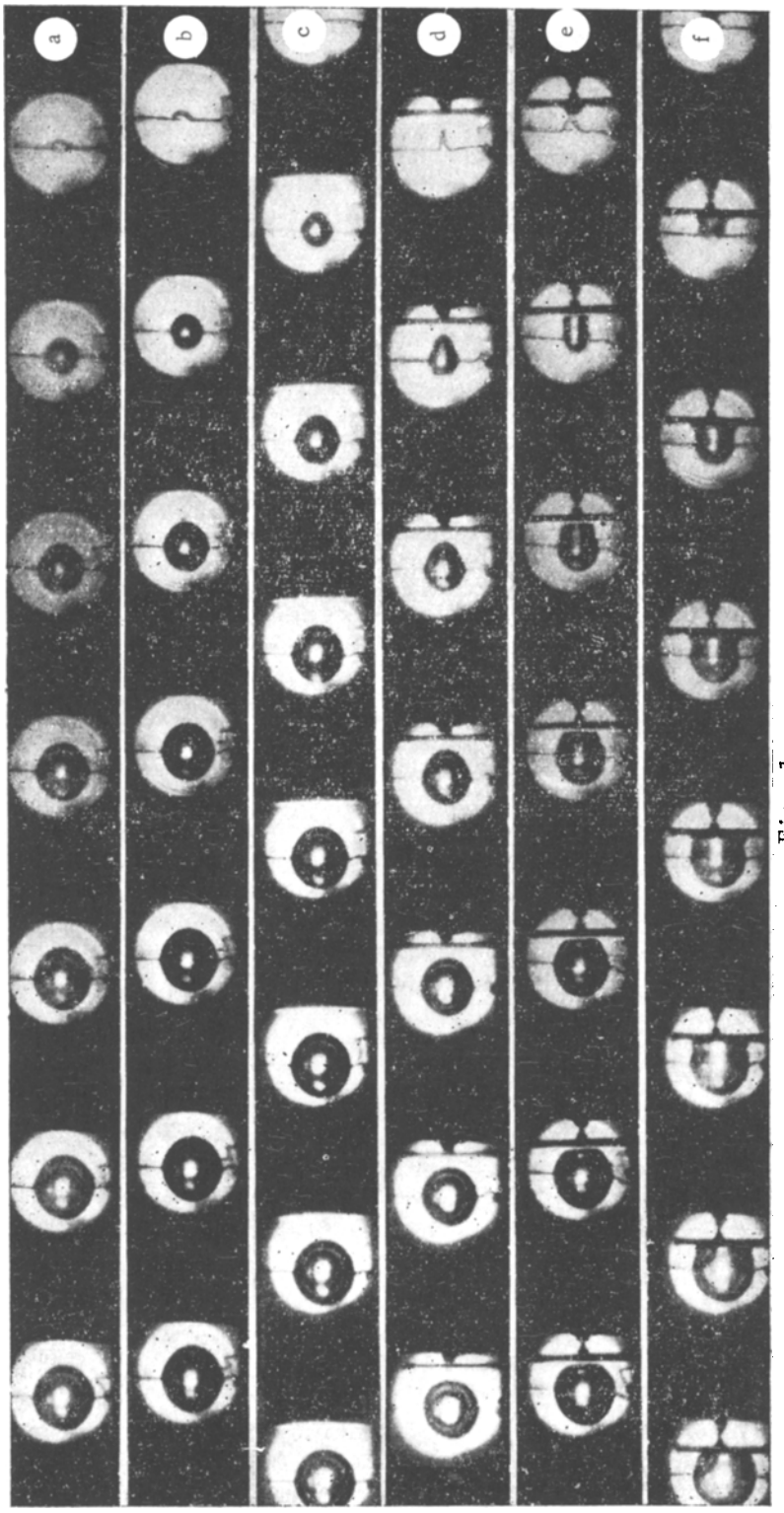

Fig. 1

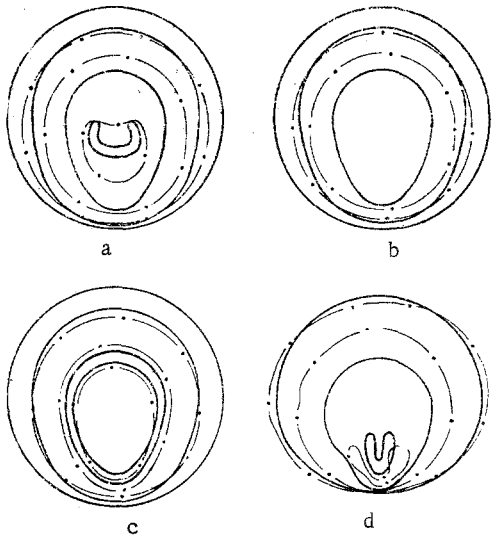

Fig. 2

As a quantitative characteristic of the deformation of the VGC during its collapse we selected (as in [9]) the eccentricity $z = (d_1 - d_2)/(d_1 + d_2)$, where d_1 and d_2 are the horizontal and vertical diameters, respectively. The relationships $z = z(b_0^*, \tau)$ are shown in Fig. 3 [Value of b_0^*: 1) 0.6; 2) 0.7; 3) 0.8; 4) 1.18; 5) 1.2; 6) 1.6; 7) 2.2]. The dashed line is Mitchell's theoretical curve [9] for $b_0^* = 1.5$.

The greatest change in eccentricity (including the change in sign at a later stage of collapse) occurs when $b_0^* < 1$. With increase in b_0^* in the region $b_0^* < 1$ the passage through zero is shifted toward larger times. For a bubble initially in contact with the wall (Fig. 3, curve 1) $z > 0$ during the whole time of collapse, and for $b_0^* > 1$ the eccentricity is negative (Fig. 3, curves 4-7).

The presented results (see Fig. 3) are graphic confirmation that a spherical VGC induced by an underwater spark near a solid plane wall ($b_0^* > 1$) becomes extended, on collapsing, along a normal to the wall, and it is not until the final stage of collapse that it again becomes spherical (dashed continuation of curves). At the same time, the cavity, which initially has the shape of a spherical segment, becomes longer initially in a direction parallel to the wall, then along a normal to it, and at the concluding stage again in a direction parallel to it. If the height of the spherical segment does not exceed 0.6, the cavity during the entire period of collapse remains extended parallel to the wall. In the concluding stage of collapse ($\tau > 0.95$) it is impossible, owing to the sharp change in shape of the cavity, to determine the behavior of $z(\tau)$ (for instance, when $b_0^* = 1.05$ the cavity at the minimum acquires a toroidal shape and the parameter z, proposed above for its characterization, becomes meaningless).

Beginning at $b_0^* > 2.2$, the curve of $z(\tau)$ asymptotically approaches zero, and when $b_0^* = 5.5$ (the curve coincides with the axis) the cavity collapses without deformation, i.e., it does not differ in any way from collapse in an unbounded volume.

A comparison (see Fig. 3) of Mitchell's theoretical curve (dashed line) with the experimental curve for $b_0^* = 1.6$ (curve 6) reveals their satisfactory agreement. Hence, the marker-and-cell technique can be used (at least when $\tau < 0.9$) for a qualitative description of the deformation of a spark-induced VGC when it collapses near a solid wall.

4. Velocity Distribution near Cavity. The reason for deformation of a cavity lies in the formation of an asymmetric velocity distribution when a solid wall is close to it. Figures 4a-c show the radial components of the cavity boundary velocity $v = \dot{R}/v_0$ [for $\theta = 0$ (a), $\pi/2$ (b), π (c); $v_0 = \sqrt{p_\infty/\rho_\infty}$; $\dot{R} = dR/dt$] as a function of time for various b_0^* [$b_0^* = 0.6$ (1), 1.1 (2), 1.6 (3), 2.2 (4), 5.5 (5), ∞ (6)]. The dashed line shows the Rayleigh solution in the absence of a wall for the collapse of an empty cavity in an incompressible liquid (θ is the angle between the radius vectors of the closest point to the wall and the considered point on the VGC surface).

A characteristic feature is that the significant difference in velocities for $\theta = \pi/2$ and π begins at $\tau \geq 0.7$, and their sharpest increase occurs when $\tau \to 1$. With increase in

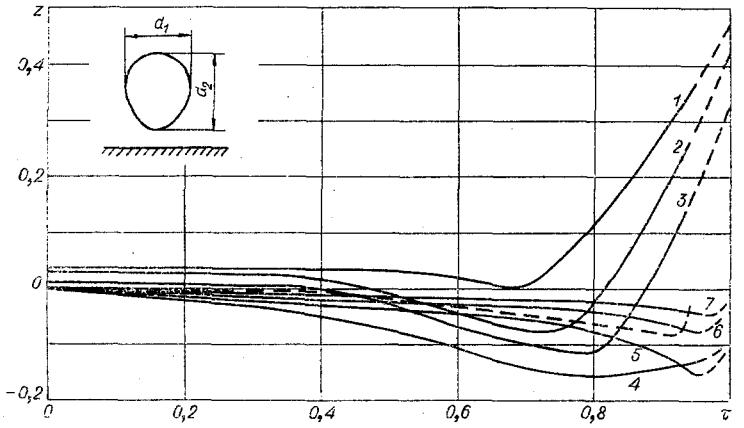

Fig. 3

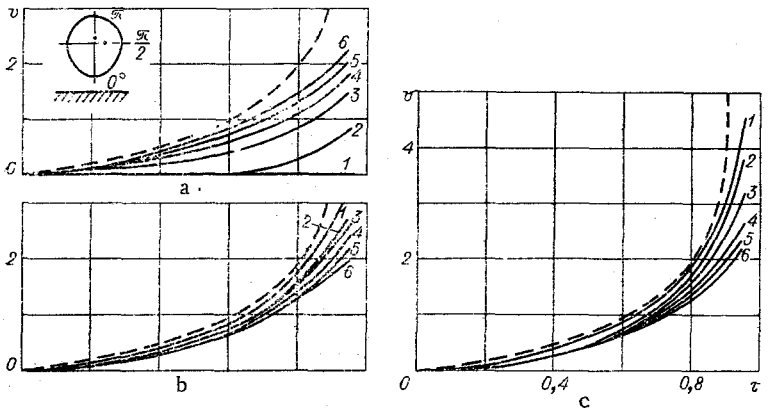

Fig. 4

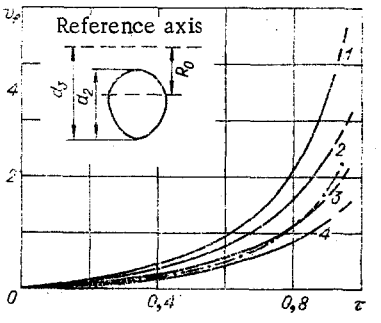

Fig. 5

b_0^* the velocity decreases and moves away from the Rayleigh curve. The obtained result indicates the erroneousness of the existing view [7, 8] that the velocity of collapse of the boundary of the VGC increases with increasing distance of it from the solid wall.

For any distance from the wall the rear boundary of the cavity has the highest velocity, which confirms the conclusion that a directed flow of liquid develops and a jet is formed. Owing to the loss of stable shape by the cavity in the conducted experiments we could not determine the time of the sharp bend in the velocity curve. For this purpose we would have to determine separately the final stage of collapse by "stretching" it in time, since the characteristics of the process attain a maximum here and are subject to the greatest changes. Such investigations, however, are beyond the scope of the problem considered here.

The motion of the front boundary of the VGC ($\theta = 0$) has several features of its own (Fig. 4a). Its velocity at any b_0^* remains lower than for $\theta = \pi/2$ or $\theta = \pi$, and increases with increase in b_0^*. When $b_0^* \geq 1.6$ the front boundary of the cavity moves synchronously with its whole surface, whereas when $b_0^* < 1.6$ the start of its motion is shifted to the right along the time axis (when $b_0^* = 1.1$ this time is 0.6). If the cavity formed near the solid surface has the shape of a truncated sphere ($0.6 < b_0^* < 1.1$) the velocity of its boundary nearest to the wall is of opposite sign (from that in the case of $b_0^* \geq 1.1$). When the cavity is at a distance $b_0^* > 5$ from the wall the velocity of its boundary (for any θ) and, hence, the motion of the flow near the cavity are practically the same as for cavity collapse in an unbounded medium.

5. Effect of Wall on Displacement of Center of Cavity and Its Collapse Time. Owing to the predominant motion of the surface furthest from the wall the center of the cavity acquires a motion directed toward the wall. As a quantitative characteristic of this motion we took the velocity of displacement of the center $v_f = \dot{f}/v_0$, where $f = [(d_3 - R_{max}) - d_2/2]/R_{max}$ is the displacement of the center, introduced by Mitchell [9] and schematically defined in the top left corner of Fig. 5 ($\dot{f} = df/dt$). Plots of the velocity of the center

against time for various b_0^* [Fig. 5, 1) $b_0^* = 0.7$; 2) 1.1; 3) 1.6; 4) 2.2] show that an appreciable movement of the center does not begin until $\tau = 0.2$. With increasing distance of the VGC from the wall the velocity of the center decreases and, beginning at $b_0^* > 5$, there is no displacement. For comparison Fig. 5 shows the calculated [9] velocity of the center for $b_0^* = 1.5$ (dashed-dot line). Comparison with the corresponding experimental curve 3 shows a satisfactory agreement.

The condition for absence of a wall effect on VGC collapse for $b_0^* > 5$ can be formulated in terms of the source parameter. It is known that the cavity energy is expressed in terms of its maximum volume by the expression

$$W_n = 4/3\pi p_\infty R^3_{\max}.$$

If we take into account that the fraction of source energy converted to cavity energy in the case of an underwater spark does not exceed 40% (50% of the discharge energy is removed by the shock wave and 10% is expended on light and heat emission), the condition for absence of an effect of the solid wall can be written in the form

$$b_0 > 5\sqrt[3]{W_0/p_\infty},$$

where $W_0 = CU_0^2/2$ is the energy stored in the capacitor bank. This inequality is enhanced, since in real conditions some of W_0 is irreversibly lost in active components of the discharge circuit (apart from the spark channel).

The maximum velocity of the cavity center (the experimental values for $\tau = 0.95$ were used) was compared with that calculated from Levkovskii's equation [5] for a model of spherically symmetric collapse

$$v_{f\max} = 17.9 b_0^{*2}\left(1 + 0.18\, b_0^*\right) x^3,$$

where

$$x = \sqrt{\frac{1+3\delta}{2}\left(1+\sqrt{1+\left(\frac{\delta}{\eta_{0\min}}\right)^3\frac{4}{(1+3\delta)^2}}\right)} + \sqrt{\frac{1+3\delta}{2}\left(1-\sqrt{1+\left(\frac{\delta}{\eta_{0\min}}\right)^3\frac{4}{(1+3\delta)^2}}\right)},$$

$$\eta_{0\min} = \frac{0.232\left(1+0.12/b_0^*\right)}{b_0^{*4/3}}.$$

The gas content $\delta = p_0/p_\infty$ of the cavity was determined from the first integral equation of motion of its boundary, written for a time τ_1 preceding the start of collapse $\tau = \tau_0 = 0$,

$$\delta = \frac{1}{2}\,\frac{(2/3)\left(R_1^{-3}-1\right) - v_1^2}{R_1^{-3}\left(R_1^{-1}-1\right)},$$

where R_1 and v_1 are the normalized radius and velocity of the cavity, respectively, determined from experiment at $\tau = \tau_1$. The adiabatic exponent of the gas, as in [5], was taken as 4/3. The results of the comparison are given in Table 1, which shows that the experimentally determined motion of the cavity toward the solid surface is 2-4 times more rapid than theory predicts. This discrepancy is probably due to the use of the very approximate reflection method [5] for the description of VGC collapse. This method provides a correct picture of the effect of distance from the wall on the maximum velocity of motion of the cavity toward it.

The cavity collapse time is greater than that calculated by Rayleigh, but the difference is insignificant (10-15%). The increase in collapse time of the cavity as it approaches the wall is due to the significant reduction of the velocity of the lower boundary of the cavity in comparison with the corresponding process in an unbounded medium. Levkovskii's equation [5] can be used for a quantitative assessment of the effect of a plane wall on the collapse time.

Thus, the development of an underwater spark at a depth exceeding $2R_{max}$ [16] and at a distance of more than $5R_{max}$ from a solid plane wall is the same as in an unbounded liquid. When these boundary surfaces are closer to the wall the special features of the process due to the

TABLE 1

b_0^*	0,7	1,1	1,2	1,6	2,2	5,5
$v_{f\,max}^{theor}$	—	1,18	1,02	0,65	0,32	0,07
$v_{f\,max}^{exp}$	5,12	2,4	2,1	1,9	1,3	0

asymmetric boundary conditions must be taken into account. The most applicable results for numerical solution of the problem can be obtained by the use of the marker-and-cell technique [9].

LITERATURE CITED

1. V. G. Stepanov, P. M. Sipilin, Yu. S. Navagin, and V. P. Pankratov, Hydroexplosive Stamping of Ship-Building Components [in Russian], Sudostroenie, Leningrad (1961).
2. M. A. Anuchin, Explosive Stamping [in Russian], Mashinostroenie, Moscow (1972).
3. G. P. Gulii, P. P. Malyushevs'kii, and M. F. Protsenko, "A powerful electric discharge in a liquid and its practical application," Visnik Akad. Nauk UkrSSR, No. 5, 66-67 (1975).
4. V. V. Voinov and O. V. Voinov, "Motion and collapse of cavities in an unbounded liquid and near a plane," Zh. Prikl. Mekh. Tekh. Fiz., No. 1, 89-95 (1975).
5. Yu. L. Levkovskii, "Collapse of a spherical gas-filled bubble near boundaries," Akust. Zh., 20, No. 1, 62-66 (1974).
6. G. A. Khoroshev, "Effect of a wall on cavity collapse," Inzh.-Fiz. Zh., 6, No. 1, 59-63 (1963).
7. A. Shima, "The behavior of a spherical bubble in the vicinity of a solid wall," Trans. ASME, Ser. D, No. 1, 75 (1968).
8. A. I. Korovkin and Yu. L. Levkovskii, "Investigation of collapse of a cavitation bubble near a solid wall," Inzh.-Fiz. Zh., 12, No. 2, 246-249 (1967).
9. T. M. Mitchell and F. G. Hammitt, "Asymmetric cavitation bubble collapse," Trans. ASME, Ser. I, No. 1, 29 (1973).
10. V. P. Vilister and M. L. Sedova, "An experimental investigation of the formation of gas cavities in a narrow gap in a liquid dielectric by low-voltage discharges," Fiz. Khim. Obrab. Mater., No. 5, 32-39 (1969).
11. S. P. Kozyrev, "Cumulative collapse of cavities produced by an electric discharge," Élektron. Obrab. Mater., No. 6, 56-62 (1969).
12. V. K. Bobolev and A. V. Dubovik, "Cumulative jets accompanying impact collapse of cavities in thin liquid layers," Zh. Prikl. Mekh. Tekh. Fiz., No. 2, 148-151 (1970).
13. C. L. Kling and F. G. Hammitt, "Photographic study of spark-induced bubble collapse," Trans. ASME, Ser. D, 94, 825 (1972).
14. V. G. Ben'kovskii, P. I. Golubnichii, and S. I. Maslennikov, "Flashes of electrodynamic sonoluminescence accompanying a high-voltage electric discharge in water," Akust. Zh., 20, No. 1, 23-26 (1974).
15. R. J. Knapp, J. W. Daily, and F. G. Hammitt, Cavitation, McGraw-Hill, New York (1970).
16. V. S. Perekval'skii, A. N. Salov, and G. V. Staver, "Experimental investigation of interaction of gas cavities formed by explosion of spherical and elongate charges under water," Fiz. Goreniya Vzryva, No. 2, 304-311 (1975).
17. V. N. Petrichenko, A. I. Vovchenko, and V. A. Burtsev, "An attachment to a high-speed camera for the investigation of processes with a duration of up to hundredths of a millisecond," Zh. Nauch. Prikl. Fotograf. Kinematograf., No. 6, 440-441 (1975).
18. V. V. Sychinskii and S. D. Beshelev, Protection of Equipment from Scale [in Russian], Mashinostroenie, Moscow (1964).